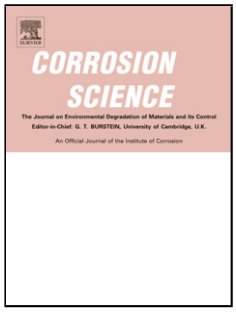

Title: Static secondary ion mass spectrometry investigation of corrosion inhibitor Irgamet®39 on copper surfaces treated in power transformer insulating oil

Author: Marco Facciotti Pedro S. Amaro Richard C.D. Brown Paul L. Lewin James A. Pilgrim Gordon Wilson Paul N. Jarman Ian W. Fletcher

PII: S0010-938X(15)00241-3
DOI: http://dx.doi.org/doi:10.1016/j.corsci.2015.05.046
Reference: CS 6333

To appear in:

Received date: 24-2-2015
Revised date: 21-5-2015
Accepted date: 22-5-2015

Please cite this article as: M. Facciotti, P.S. Amaro, R.C.D. Brown, P.L. Lewin, J.A. Pilgrim, G. Wilson, P.N. Jarman, I.W. Fletcher, Static secondary ion mass spectrometry investigation of corrosion inhibitor Irgamet*regd*39 on copper surfaces treated in power transformer insulating oil, *Corrosion Science* (2015), http://dx.doi.org/10.1016/j.corsci.2015.05.046

Highlights

- SSIMS was used to study corrosion inhibition of copper treated in insulating oil.
- Desorption experiments allowed the study of the inhibitor stability in vacuum.
- The energy of desorption of tolyltriazole under SSIMS conditions was calculated.
- SSIMS imaging was shown to be an applicable new diagnostic tool for transformers.

Static secondary ion mass spectrometry investigation of corrosion inhibitor Irgamet®39 on copper surfaces treated in power transformer insulating oil

Marco Facciotti*[a], Pedro S. Amaro[b], Richard C. D. Brown*[a], Paul L. Lewin[b], James A. Pilgrim[b], Gordon Wilson[c], Paul N. Jarman[c] and Ian W. Fletcher[d]

[a] Department of Chemistry, University of Southampton, Southampton SO17 1BJ, UK.
[b] Tony Davies High Voltage Laboratory, University of Southampton, Southampton SO17 1BJ, UK.
[c] National Grid, National Grid House, Warwick Technology Park, Gallows Hill, Warwick CV34 6DA, UK.
[d] Intertek Wilton, The Wilton Centre, Redcar TS10 4RF, UK.
*E-mail: facciotti.marco@gmail.com**;** R.C.Brown@soton.ac.uk
Phone: +44(023) 8059 4108
Address: Department of Chemistry, University of Southampton, University Road, Highfield, Southampton SO17 1BJ, UK.

Abstract

Static secondary ion mass spectrometry was used to study the corrosion inhibitor Irgamet®39 on the surface of copper treated in insulating oils and the effect of temperature changes, by means of temperature programmed desorption experiments under vacuum, on metal coverage. Four commercial oils, both corrosive and non-corrosive, showed no significant influence on the stability of the tolyltriazole layer and the energy of its main desorption event from copper was calculated around 100 kJ mol^{-1}. Finally, an example of ion imaging as diagnostic tool to track the distribution of corrosion inhibitor and by-products in decommissioned or failed power transformers is described.

Highlights

- SSIMS was used to study corrosion inhibition of copper treated in insulating oil.
- Desorption experiments allowed the study of the inhibitor stability in vacuum.
- The energy of desorption of tolyltriazole under SSIMS conditions was calculated.
- SSIMS imaging was shown to be an applicable new diagnostic tool for transformers.

Keywords

A. copper; A. organic coatings; B. SIMS; C. sulphidation.

Introduction

The field of high voltage engineering has its origins in the requirement for high performance of electrical distribution networks, which face continually growing demands for capacity and resilience. Every electrical distribution network relies on some strategic assets such as transformers. Most transformers in use today throughout the world are filled with mineral oil, complying with international standards (e.g. IEC 60296), for the dual purpose of providing electrical insulation and cooling of the copper conductors [1,2]. Sulphide-mediated corrosion of copper and its alloys is a known issue in many applications of metallic materials, still subject of interest of the corrosion scientific community in both aqueous [3–6] and non aqueous environment [7–10]. In fact, previous studies have shown how certain organic compounds containing sulphur (e.g. dibenzyl disulphide, DBDS) [11] are able to chemically attack copper surfaces immersed in insulating mineral oil causing metal displacement, promoted by oxygen, together with the formation of corrosive by-products such as copper sulphides (Cu_xS) [12–15]. Copper sulphides, being ionic compounds, can interfere with the insulation system (solid and liquid components) reducing its reliability; this can result in catastrophic failure of high voltage assets, power distribution disruption and, ultimately, reputational and financial losses [16–18]. To protect these valuable and essential pieces of equipment from 'corrosive sulphur' species the most common prevention and mitigation strategy is the addition of an organic corrosion inhibitor to the oil [2,19].

A corrosion inhibitor is a molecule, which binds to metallic surface with high affinity, capable of retarding or preventing attack of corrosive compounds [20]. Benzotriazole (BTA) and its derivatives are among the most effective copper corrosion inhibitors [10,21–24]. The protective film formed by BTA derivatives on copper surfaces may function both as a physical barrier to ionic or reactive species, and to attenuate copper dissolution [25]. Evidence of the presence of tolyltriazole on copper treated in oil was previously shown using Time of Flight Secondary Ion Mass Spectrometry (ToF-SIMS) [26,27], but contextual estimation of its thermal stability were never reported.

The addition of an organic corrosion inhibitor is preferred, in power transformer applications, over other mitigation strategies (e.g. oil reclamation, selective depolarization or substitution) due to its efficacy and relatively low cost [2,28]. Irgamet®39, a mixture of methyl-BTA isomers (Figure 1), is the most widely used corrosion inhibitor to protect copper conductors [29]. It comprises a methyl-BTA (tolyltriazole) moiety and a secondary aliphatic amine moiety; the first is actively involved in the protection, after being released via retro-Mannich reaction [19,29], whilst the latter serves to solubilize the tolyltriazole in the oil (Fig. 1). Upon addition of the corrosion inhibitor any damage to the copper surfaces or contamination of the oil or paper insulation remain unchanged, although further degradation may be prevented [19].

In fact, organic inhibition of copper is not a permanent solution and degradation of corrosion inhibitor performance is a well-known issue, due to the effects of high temperatures and chemical reactions [30]. Literature studies of the thermal and chemical stability of BTA derivatives on copper surfaces in oil indicate some divergence of opinions. In common with other BTA derivatives, Irgamet®39 is known to undergo some degradation in the presence of hydroperoxides, most likely formed via hydrocarbon peroxidation reactions.

However, some researchers consider this degradation mechanism almost insignificant in transformers [19,29]. Empirical studies reported effective corrosion inhibition even under the worst simulated operational conditions [16,31]. On the other hand, others concluded that the same severe thermal conditions that promote the formation of the corrosion by-products (i.e. copper sulphides), also promote the degradation of tolyltriazole-based corrosion inhibitors, rendering them ineffective [32]. Effective corrosion inhibition strongly depends on the quality of the metal surface, therefore it was postulated that a corroded copper surface may exhibit reduced adsorption [33]. In any case, the long-term effectiveness of such inhibition still remains unknown [2,34], and it should only be considered as a mitigation strategy.

Herein we report the results of a study towards the evaluation of temperature programmed desorption static secondary ion mass spectrometry (TPD-SSIMS) as analytical tool to study corrosion inhibition of copper surfaces produced in insulating oil environments. This technique is particularly well-suited to the study of organic overlayers at metal surfaces due to its unique molecular selectivity, through the observation of emitted molecular or fragment ions characteristic of the organic corrosion inhibitor molecule [35]. In the present study, desorption of the corrosion inhibitor is conveniently visualised as a series of colour-coded images collected as the samples undergo a controlled heating ramp across a range of temperatures. These desorption data together with theoretical calculations of the binding energies allow estimation of the thermal stability and desorption behaviour of the corrosion inhibitor under vacuum. Finally, an application of SSIMS imaging to track the distribution of corrosion inhibitor and corrosion by-products on copper taken from a scrapped transformers is provided.

Materials and methods

Solution and surface preparation

Oils used were Base oil 20 (SPEXCertiPrep, Inc.) and the three commercial transformer naphtenic mineral oils Nytro Gemini X (Nynas AB), HyVolt III (Ergon Inc.) and Nytro 10GBN (Nynas AB). Gemini X and HyVolt III are inhibited mineral oils while 10GBN is uninhibited and naturally corrosive, characterised by typical aromatic content of 3%, 9% and 14% respectively. All oils were free from detectable DBDS and corrosion inhibitors and were used without degassing. Typically, they show water content < 30 ppm and acidity < 0.01 mg KOH g^{-1}.

All oil samples at 100 ppm (concentration commonly used in industry [28]) of Irgamet®39 (BASF) were prepared using dilutions, by weight, of the respective stock solutions at 1000 ppm. Stock solutions were prepared from 50 g of each oil with the addition of 50 mg of Irgamet®39. Final solutions were the result of a 1:10 dilution, by weight, to 10 g. Oxygen free high conductivity (OFHC, Siemens) copper transformer conductor samples were used. Copper samples, were cut to a size of ~100 mm^2 and unwrapped to remove the layers of insulating paper immediately before the start of the experiment. Copper samples were then washed with fresh cyclohexane and placed in 20 mL headspace glass vials containing the oil solutions, closed with

butyl/PTFE septa crimp seals and treated at 70 °C for 24 hours in a fan oven. The solvent rinse prior to the experiment was deemed necessary to thoroughly degrease the metal surface from contaminants, avoiding its exposure to an aqueous environment. Samples were then removed from the oil, washed three times with fresh cyclohexane to remove all oil traces and stored in screw-top glass vials. New glass vials and disposable pipettes were used during the sample preparation, all handling was performed with clean nitrile gloves and stainless steel tweezers at all times.

TPD-SSIMS analysis

Samples described in this work were analyzed by Static SIMS using the Ion-ToF 'ToFSIMS IV' instrument. The copper samples were attached to a suitable sample holder using clean metal clips. The samples for analysis were handled using clean stainless steel tweezers at all times. For the SSIMS work, positive and negative ion spectra were recorded with 200 μm x 200 μm analysis areas. The total ion dose for each acquisition was ≈ 5 x 10^{11} ions cm^{-2}. This was within the accepted ion dose limit for static SIMS of 5 x 10^{12} ions cm^{-2}. The Bi_3^{2+} ion source was used in all cases reported. Data were recorded from the samples using the 'bunched' mode of operation. The spatial resolution achieved in the images was ≈ 4 μm and the mass resolution, m/Δm, was around 5000. Reference spectra for the liquid samples were collected by analyzing the pure liquid spread as a thin layer on clean PET film. Samples for thermal desorption analysis were mounted individually on to a 'main chamber heating/cooling' sample holder under a clean Mo grid (see Supplementary Material). The thermocouple used to measure the sample temperature was trapped between the sample surface and the underside of the Mo grid. For the thermal desorption work, the sample was stabilized at the starting temperature of 27 °C (300 K) for approximately 10 minutes. The profile acquisition was started and the temperature ramp (5 degrees per minute) began after 20 s acquisition time. The profiling was stopped manually at 400 °C (673 K). The main chamber pressure during analysis was less than ≈ 5 x 10^{-7} mbar from a base pressure of ≈ 5 x 10^{-9} mbar. Negative ion thermal desorption profiles, images and spectra were recorded from fresh areas of the samples using a 500 μm^2 analysis area in each case. The total ion dose for each profile was ≈ 2 x 10^{12} ions cm^{-2}, which was within the accepted ion dose limit for static SIMS of 5 x 10^{12} ions cm^{-2}. Data were recorded from the samples using the 'bunched' mode of operation. The spatial resolution achieved in the images was ≈ 4 μm and the mass resolution, m/Δm, was around 5000. The profiles and images were recorded using the 'raw' data stream mode (RAW).

Energy of Desorption (E_{des}) calculations

Data were reprocessed in order to plot intensity vs. time for the representative ion at m/z = –132. Data were exported from the instrument 'IonSpec' software in ASCII format and then processed using Excel2000 and Origin 9.1. 5 points FFT and adjacent averaging smoothing (100 points) was used to reduce the data noise at low temperature and the first derivative plots were obtained. Data processing details can be found in the Supplementary Material. The temperature at maximum desorption rate (T_p) is then used to calculate the energy

of desorption into vacuum (E_{des}) assuming a first order process and absence of intramolecular interactions and re-adsorption. The equation used is shown below [36].

$$E_{des} = T_p R\left[\ln\left(\frac{\nu_i T_p}{B}\right) - 3.64\right] \qquad \text{(Eq. 1)}$$

where B is the heating rate (5 K min^{-1} = 0.08333 K s^{-1}) and ν_i is the rate constant (10^{13} s^{-1}).

Results and discussion

Initially, to establish an experimental routine, a clean base oil model system (Base Oil 20) was used. Additionally, three representative commercial insulating oils used in high voltage power transformers were investigated: Nytro Gemini X, HyVolt III and Nytro 10GBN (known to be corrosive). Secondary ion mass spectra collected from the oil samples were consistent with highly refined oil products for insulating applications. Although a significant part of the results shown here are from samples treated in Gemini X, the discussion can be extended to all other samples. The complete set of results for all samples can be found in the Supplementary Material.

TPD-SSIMS profiles

For each of the samples, an intensity profile of the major secondary ions of interest was obtained across the temperature range and their complete mass assignment is available in the Supplementary Material. Secondary ion temperature desorption profiles for copper treated with 100 ppm of Irgamet®39 in Gemini X are presented in Fig. 2 and Fig. 3. The relative secondary ion yield from the surface of the sample was observed to vary significantly with increasing temperature. Low amounts of $^{63}Cu^-$ ions are observed to be steadily emitted from the metal substrate across the entire range of temperatures investigated (Fig. 2). Chloride ion, from environmental contamination of the metal, is observed to be substantially depleted at ca. 100 °C. A similar profile is observed for $Cu(CN)_2^-$ ions, formed through combination of ionised/excited Cu atoms with organic fragments of the corrosion inhibitor. Conversely, cyanide ion is observed to increase above 100 °C, suggesting the breakdown of $Cu(CN)_2^-$, decreasing again above ca. 130 °C as the corrosion inhibitor is depleted (Fig. 2). More interesting and relevant to the study of corrosion inhibition of copper in insulating oils are ions directly related to Irgamet®39 (Fig. 3). The molecular ion in negative polarity mode representative of the surface-active moiety of the corrosion inhibitor molecule ($[M–H]^-$) is a deprotonated tolyltriazole at m/z = –132, $[C_7H_6N_3]^-$, which is also the most abundant ion in the set followed by its main fragmentation product at m/z = –68, $[C_2H_2N_3]^-$, a deprotonated triazole. Interestingly, metaphosphate ion ($[PO_3]^-$), indicative of the presence of oxidized phosphorus on the metal surface, was also observed for all oil-treated samples, and was the predominant ion for samples treated in Base Oil 20. The source of these oxidized P-containing species is likely due to blending of phosphorus-based secondary antioxidants, such as triarylphosphite-based hydroperoxide deactivators commonly used in lubricant and polymer applications [37]. Indeed, SIMS analysis on all samples treated in transformer oils showed traces of characteristic ions for tris(2,4-di-*tert*-butylphenyl) phosphite, again highlighting the power of the technique. Base Oil 20 did not show specific markers for the presence of such

species although, as every base oil product subject to severe hydro treatment that destroys any natural inhibition, it is far more likely to contain antioxidant additives [38]. Regardless of their origin, oxidized P-containing species are present on the surface of copper following exposure to the oils.

For most samples it was possible to see at least two distinct desorption events for tolyltriazole (m/z = –132 and m/z = –68, Fig. 4), which could indicate desorption from different copper sites as temperature increases (e.g. crystallographic facets).

Although it is not possible to provide a quantitative measurement of the amount of corrosion inhibitor present on the surface of the metal of each of the samples, a comparison of the thermal stability of the corrosion inhibitor layer under ultra-high vacuum conditions can be made. A comparison of the thermal profiles for the tolyltriazole negative ion (m/z = –132) on samples aged in different oils is reported (Fig. 5). Under ultra-high vacuum conditions, the thermal desorption is completed by ca. 105 °C for all samples. An apparently reduced stability of tolyltriazole is observed for the layer formed in Base Oil 20, where surface oxidized phosphorus species may disrupt normal action of the corrosion inhibitor. The variability of absolute intensity of secondary ion yield, observed between samples resulted from minor variations of instrument operating parameters and the nature of the sample (corrosion inhibitor coverage, topography, composition or oxidation state of the surface) and represents an intrinsic reproducibility limitation of the technique.

Ion imaging

Ion imaging provides a visual description of the effect of increasing the temperature of copper upon the corrosion inhibitor layer. For clarity, only two representative ions are illustrated, $^{63}Cu^-$ (red) and $[C_7H_6N_3]^-$, m/z = –132 (green). The total ion image, displaying the surface topography, is also shown in grey scale. Data collected from the sample treated in Gemini X are reported (Fig. 6), and show qualitatively how the corrosion inhibitor layer is readily desorbed at T > 105 °C.

It is important to note that desorption of tolyltriazole occurs more readily and irreversibly under the ultra-high vacuum conditions of the SSIMS experiment. These conditions differ significantly from those of an operational transformer, where equilibrium exists between corrosion inhibitor absorbed on the surface and in the oil. Therefore, desorption temperatures observed in the TPD-SSIMS should not be directly extrapolated to real transformers.

Inspection of the tolyltriazole molecular ion (m/z = –132) signal intensity between 40 °C and 100 °C provides a quantitative assessment of the desorption process, showing how corrosion inhibitor coverage is influenced as the temperature of copper changes (Fig. 7).

The tolyltriazole is most readily desorbed from the sample treated with Irgamet®39 in Base Oil 20, where the intensity of the tolyltriazole molecular ion decreased more rapidly across the temperature range investigated. As discussed above, this may be related to the presence of surface phosphorus species, especially in Base Oil 20, capable of affecting the corrosion inhibitor layer stability. The three commercial insulating mineral oils Gemini X, HyVolt III and the corrosive oil 10GBN exhibited similar desorption profiles, although the first

appears to have higher corrosion inhibitor coverage in the range 80-90 °C, followed by samples treated in 10GBN and HyVolt III respectively.

Energy of desorption (E_{des}) calculation

Energy of desorption is the energy required to break the interaction between tolyltriazole and the copper surface. The results of the energy calculations, using Redhead's model [36], for the main desorption events are shown for samples prepared in the different oils (Table 1). For all samples analyzed, E_{des} was calculated, by means of Eq. 1, to be between 99 kJ mol^{-1} and 103 kJ mol^{-1} that is in the range of DFT predicted values for similar systems in vacuum [39,40]. This energy is substantially lower than typical covalent bond energies such as C-C (347 kJ mol^{-1}), C-N (305 kJ mol^{-1}), C=C (614 kJ mol^{-1}) and N=N (418 kJ mol^{-1}) [41]. This is consistent with a desorption event rather than molecular decomposition, which is supported by the observation of tolyltriazole molecular ion (m/z = –132). The maximum value is found for the sample treated in Gemini X while the minimum for that treated in Base Oil 20.

Table 1. Energy of desorption of tolyltriazole on copper treated in different oils[a].

Sample	T_p [°C]	E_{des} [kJ mol^{-1}]
Base Oil 20	72	99
Gemini X	86	103
HyVolt III	76	100
10GBN	75[b]	100

[a] Calculated using Eq. 1 using the temperature at maximum desorption rate (T_p) assuming a first order process and absence of intramolecular interactions and re-adsorption. T_p was defined as that at the minimum of the 1st differential of the corresponding TPD-SSIMS profile. [b] Two comparable minima in the first differential were found therefore an average T_p value was used.

However, at least using this simplistic approach to the calculation, the nature of the oil in which the corrosion inhibitor is used has relatively little effect on calculated E_{des}. A larger effect on E_{des} would be expected in the case of substantial surface modification.

Application of SSIMS imaging to transformer windings

SSIMS imaging was applied to track the distribution of tolyltriazole across the copper windings of a scrapped transformer that had been treated with Irgamet®39 during service [42]. The transformer was known to have suffered from overheating issues in the upper half of its windings. Two samples were taken from upper (Fig. 8b) and lower (Fig. 8c) parts of a copper winding of a 400/275 kV transformer and results are reported below. The upper and lower winding samples from the transformer look very different from the reference material prepared in the laboratory, which is characterized by the uniform coverage of tolyltriazole on the surface of copper with no traces of the underlying metal or sulphur-related corrosion by-products (Fig. 8a). The sample

collected from the upper part of the winding shows almost no contribution from the tolyltriazole ions, indicating the destruction of the corrosion inhibitor layer due to thermal stress. Areas of exposed metal and sulphur-rich flaky formations are also obvious in the image, indicating advanced corrosion. By contrast, the sample collected from the lower part of the transformer winding, where the temperature in service was lower, is in a less advanced state of corrosion, without evidence of bare copper. The overall turquoise appearance of the image (Fig. 8c) derives from combination of blue and green pixels, representative of significant contributions from sulphur corrosion by-products together with tolyltriazole from the corrosion inhibitor layer.

Conclusions

SSIMS has been applied to identify molecular species absorbed at the surface of copper samples that have undergone corrosion inhibition with Irgamet®39 in insulating transformer oils. The molecular ion (m/z = –132) representative of the active tolyltriazole corrosion inhibitor was observed in all samples. SSIMS also revealed metaphosphate as a secondary ion, which is indicative of the formation of surface phosphorus oxides possibly derived from antioxidant impurities present, especially in Base Oil 20. Phosphorous species had not been detected on copper during previous surface analysis in our laboratory using either XRF or XPS, highlighting once again the unique contribution of SSIMS to the study of the process.

TPD-SSIMS was used to perform variable temperature ion imaging of the inhibited metal surfaces, allowing a visual qualitative description of the desorption processes. A simple model was used for E_{des} calculations, under ultra-high vacuum conditions, for tolyltriazole on copper surfaces treated in different insulating oils. In all cases, the main desorption event was found corresponding to E_{des} around 100 kJ mol^{-1}.

Finally, it was shown that SSIMS imaging can provide a useful diagnostic tool to track the distribution of corrosion inhibitor and corrosion by-products on copper conductors taken from decommissioned or failed transformers.

Supplementary Material

Oil mass spectra and m/z assignments, data for control samples, ion thermal profiles and surface ion imaging, first derivative plots for m/z = –132 for E_{des} calculations, details of the TPD sample holder.

Acknowledgements

The authors gratefully thank National Grid for the financial support to the project. MF thanks BASF for providing Irgamet®39 and Dr H. Ding (Doble Engineering Company) for the collection of the transformer samples. Dr A. Kokalj (Jožef Stefan Institute) is also thanked for helpful discussions.

References

[1] M.J. Heathcote, The J & P transformer book: a practical technology of the power transformer, Newnes, 2007.

[2] M. Dahlund, I. Atanasova-Höhlein, R. Maina, N. Dominelli, T. Ohnstad, T. Amimoto, et al., CIGRE WG A2-32 Copper sulphide in transformer insulation Final Report, 2009.

[3] B.M. Thethwayo, A.M. Garbers-Craig, Laboratory scale investigation into the corrosion of copper in a sulphur-containing environment, Corros. Sci. 53 (2011) 3068–3074. doi:10.1016/j.corsci.2011.05.016.

[4] T.T.M. Tran, C. Fiaud, E.M.M. Sutter, Oxide and sulphide layers on copper exposed to H2S containing moist air, Corros. Sci. 47 (2005) 1724–1737. doi:http://dx.doi.org/10.1016/j.corsci.2004.08.019.

[5] T.T.M. Tran, C. Fiaud, E.M.M. Sutter, A. Villanova, The atmospheric corrosion of copper by hydrogen sulphide in underground conditions, Corros. Sci. 45 (2003) 2787–2802. doi:http://dx.doi.org/10.1016/S0010-938X(03)00112-4.

[6] A. Drach, I. Tsukrov, J. DeCew, J. Aufrecht, A. Grohbauer, U. Hofmann, Field studies of corrosion behaviour of copper alloys in natural seawater, Corros. Sci. 76 (2013) 453–464. doi:10.1016/j.corsci.2013.07.019.

[7] R.D. Armstrong, C.A. Hall, The corrosion of metals in contact with ester oils at temperatures up to 200°C., Corros. Sci. 36 (1994) 463–477. doi:10.1016/0010-938X(94)90037-X.

[8] M.A. Fazal, A.S.M.A. Haseeb, H.H. Masjuki, Corrosion mechanism of copper in palm biodiesel, Corros. Sci. 67 (2013) 50–59. doi:10.1016/j.corsci.2012.10.006.

[9] Y. Qian, W. Su, Research on influencing factors of corrosive sulfur attacking copper in insulating oil and prevention, IEEJ Trans. Electr. Electron. Eng. 8 (2013) 546–549. doi:10.1002/tee.21894.

[10] M. Levin, P. Wiklund, C. Leygraf, Bioorganic compounds as copper corrosion inhibitors in hydrocarbon media, Corros. Sci. 58 (2012) 104–114. doi:10.1016/j.corsci.2012.01.009.

[11] M.C. Bruzzoniti, R.M. De Carlo, C. Sarzanini, R. Maina, V. Tumiatti, Stability and Reactivity of Sulfur Compounds against Copper in Insulating Mineral Oil: Definition of a Corrosiveness Ranking, Ind. Eng. Chem. Res. 53 (2014) 8675–8684. doi:10.1021/ie4032814.

[12] M. Facciotti, P.S. Amaro, A.F. Holt, R.C.D. Brown, P.L. Lewin, J.A. Pilgrim, et al., Contact-based corrosion mechanism leading to copper sulphide deposition on insulating paper used in oil-immersed electrical power equipment, Corros. Sci. 84 (2014) 172–179. doi:10.1016/j.corsci.2014.03.024.

[13] R. Maina, V. Tumiatti, M. Pompili, R. Bartnikas, Corrosive sulfur effects in transformer oils and remedial procedures, IEEE Trans. Dielectr. Electr. Insul. 16 (2009) 1655–1663. doi:10.1109/tdei.2009.5361586.

[14] F. Scatiggio, V. Tumiatti, R. Maina, M. Tumiatti, M. Pompili, R. Bartnikas, Corrosive Sulfur Induced Failures in Oil-Filled Electrical Power Transformers and Shunt Reactors, IEEE Trans. Power Deliv. 24 (2009) 1240–1248. doi:10.1109/tpwrd.2008.2005369.

[15] V. Tumiatti, C. Roggero, M. Tumiatti, S. Di Carlo, R. Maina, State of the art in quantification of DBDS and other corrosive sulfur compounds in unused and used insulating oils, IEEE Trans. Dielectr. Electr. Insul. 19 (2012) 1633–1641.

[16] J.M. Lukic, S.B. Milosavljevic, A.M. Orlovic, Degradation of the Insulating System of Power Transformers by Copper Sulfide Deposition: Influence of Oil Oxidation and Presence of Metal Passivator, Ind. Eng. Chem. Res. 49 (2010) 9600–9608. doi:10.1021/ie1013458.

[17] F. Scatiggio, M. Pompili, R. Bartnikas, Oils with presence of corrosive sulphur - Migration and collateral effects, 2009 IEEE Electr. Insul. Conf. (2009).

[18] M.C. Bruzzoniti, R.M. De Carlo, C. Sarzanini, R. Maina, V. Tumiatti, Determination of copper in liquid and solid insulation for large electrical equipment by ICP-OES. Application to copper contamination assessment in power transformers., Talanta. 99 (2012) 703–11. doi:10.1016/j.talanta.2012.07.009.

[19] P. Wiklund, M. Levin, B. Pahlavanpour, Copper Dissolution and Metal Passivators in Insulating Oil, IEEE Electr. Insul. Mag. 23 (2007) 6–14. doi:10.1109/MEI.2007.386479.

[20] L.R. Lewand, Passivators, Neta World. (2006) 1–3.

[21] M. Finšgar, I. Milošev, Inhibition of copper corrosion by 1,2,3-benzotriazole: A review, Corros. Sci. 52 (2010) 2737–2749. doi:10.1016/j.corsci.2010.05.002.

[22] N.K. Allam, A.A. Nazeer, E.A. Ashour, A review of the effects of benzotriazole on the corrosion of copper and copper alloys in clean and polluted environments, J. Appl. Electrochem. 39 (2009) 961–969. doi:10.1007/s10800-009-9779-4.

[23] J.A. Waynick, The development and use of metal deactivators in the petroleum industry: A review, Energy & Fuels. 15 (2001) 1325–1340. doi:10.1021/ef010113j.

[24] M.B. Antonijevic, M. M., Petrovic, Copper Corrosion Inhibitors. A review, Int. J. Electrochem. Sci. 3 (2008) 1–28. http://www.electrochemsci.org/papers/vol3/3010001.pdf (accessed March 24, 2014).

[25] K. Mansikkamäki, P. Ahonen, G. Fabricius, L. Murtomäki, K. Kontturi, Inhibitive Effect of Benzotriazole on Copper Surfaces Studied by SECM, J. Electrochem. Soc. 152 (2005) B12. doi:10.1149/1.1829413.

[26] T. Amimoto, E. Nagao, J. Tanimura, S. Toyama, N. Yamada, Duration and mechanism for suppressive effect of triazole-based passivators on copper-sulfide deposition on insulating paper, IEEE Trans. Dielectr. Electr. Insul. 16 (2009) 257–264. doi:10.1109/tdei.2009.4784575.

[27] M. Levin, P. Wiklund, H. Arwin, Adsorption and film growth of N-methylamino substituted triazoles on copper surfaces in hydrocarbon media, Appl. Surf. Sci. 254 (2007) 1528–1533. doi:10.1016/j.apsusc.2007.07.023.

[28] B. Lukic, J., Gupta, T.C.S.M., Wilson G., Scatiggio, F., Maina, R., Amimoto, T., Atanasova-Höhlein, I., Smith, P., Bertrand, Y., Skholnik, A., Friedenberg de Lemos, L.E., Lewand, L., Perrier, C., Grisaru, M., Rasco, J., Dorieux, S., Lombard, A., Piexoto, A., CIGRE WG A2-40 Copper sulphide long-term mitigation and risk assessment, 2013.

[29] P. Wiklund, Chemical stability of benzotriazole copper surface passivators in insulating oils, Ind. Eng. Chem. Res. 46 (2007) 3312–3316. doi:10.1021/ie061570w.

[30] M.A.G. Martins, A.R. Gomes, B. Pahlavanpour, Experimental study of a passivated oil corrosiveness, after depletion of the passivator, IEEE Electr. Insul. Mag. 25 (2009) 23–27. doi:10.1109/mei.2009.5313707.

[31] T. Wan, H. Qian, Z. Zhou, S.K. Gong, X. Hu, B. Feng, Suppressive mechanism of the passivator Irgamet 39 on the corrosion of copper conductors in transformers, IEEE Trans. Dielectr. Electr. Insul. 19 (2012) 454–459. <Go to ISI>://WOS:000303069300011.

[32] R. Maina, V. Tumiatti, F. Scatiggio, M. Pompili, R. Bartnikas, Transformers Surveillance Following Corrosive Sulfur Remedial Procedures, IEEE Trans. Power Deliv. 26 (2011) 2391–2397. doi:10.1109/tpwrd.2011.2157177.

[33] F. Kato, T. Amimoto, R. Nishiura, K. Mizuno, S. Toyama, Suppressive effect and its duration of triazole-based passivators on copper sulfide deposition on kraft paper in transformer, IEEE Trans. Dielectr. Electr. Insul. 20 (2013) 1915–1921. doi:10.1109/TDEI.2013.6633725.

[34] M.A.G. Martins, A.R. Gomes, Experimental study of the role played by DBDS in insulant oil corrosivity - Effect of passivator Irgamet 39, IEEE Electr. Insul. Mag. 26 (2010) 27–32.

[35] C.M. Mahoney, Surface analysis of organic materials with polyatomic prymary ion sources, in: C.M. Mahoney (Ed.), Wiley Ser. Mass Spectrom. - Clust. Second. Ion Mass Spectrom. Princ. Appl., Somerset, NJ, USA, 2013: p. 366. Retrieved from http://www.ebrary.com.

[36] P.A. Redhead, Thermal desorption of gases, Vacuum. 12 (1962) 203–211. doi:10.1016/0042-207X(62)90978-8.

[37] L.R. Rudnick, Lubricant Additives: Chemistry and Applications, in: Second, CRC Press, 2009: pp. 7–8, 28–29. https://books.google.co.uk/books?id=IQW4eCMPuxoC&dq=phosphite+secondary+antioxidants+lubricant&hl=it&source=gbs_navlinks_s.

[38] Nynas AB, Base Oil Handbook, 2001. http://www.engnetglobal.com/documents/pdfcatalog/NYN001_200412073535_Base oil handbookENG.pdf.

[39] S. Peljhan, A. Kokalj, DFT study of gas-phase adsorption of benzotriazole on Cu(111), Cu(100), Cu(110), and low coordinated defects thereon., Phys. Chem. Chem. Phys. 13 (2011) 20408–17. doi:10.1039/c1cp21873e.

[40] S. Peljhan, J. Koller, A. Kokalj, The Effect of Surface Geometry of Copper on Adsorption of Benzotriazole and Cl. Part I, J. Phys. Chem. C. 118 (2014) 933–943. doi:10.1021/jp409717e.

[41] S.S. Zumdhal, S.A. Zumdhal, Covalent Bond Energies and Chemical Reactions, in: Chemistry (Easton)., 9TH ed., Brooks/Cole Publishing Co., 1999: p. 1143.

[42] M. Facciotti, P.S. Amaro, R.C.D. Brown, P.L. Lewin, J.A. Pilgrim, G. Wilson, et al., Passivators, corrosive sulphur and surface chemistry. Tools for the investigation of effective protection, in: MyTransfo 2014 Oil Transform., 2014: pp. 27–35.

Figure captions

Fig. 1: Proposed binding model for Irgamet®39 on copper following retro-Mannich reaction.

Fig. 2: TPD-SSIMS profiles ($^{63}Cu^-$, Cl^-, CN^- and $Cu(CN)_2^-$) for copper treated with 100 ppm of Irgamet®39 in Gemini X at 70 °C for 24 hours.

Fig. 3: TPD-SSIMS profiles (triazole ($[C_2H_2N_3]^-$), tolyltriazole ($[C_7H_6N_3]^-$), PO_3^- and Cu complexes) for copper treated with 100 ppm of Irgamet®39 in Gemini X at 70 °C for 24 hours.

Fig. 4: TPD-SSIMS profiles for triazole ($[C_2H_2N_3]^-$, m/z = –68) and tolyltriazole ($[C_7H_6N_3]^-$, m/z = –132) for copper treated with 100 ppm of Irgamet®39 in Gemini X at 70 °C for 24 hours.

Fig. 5: Comparison of TPD-SSIMS profiles of tolyltriazole negative ion ($[C_7H_6N_3]^-$) for copper samples treated with 100 ppm of Irgamet®39 in different oils at 70 °C for 24 hours.

Fig. 6: Ion images from a copper surface (500 μm^2) treated with 100 ppm of Irgamet®39 in Gemini X (70 °C, 24 hours) exposed to different temperatures showing m/z = –132 (green) and m/z = –63 (red). (For interpretation of the references to colour in this figure, the reader is referred to the web version of this article.)

Fig. 7: Tolyltriazole molecular ion (m/z = –132) surface signal or corrosion inhibitor coverage variation between 40 °C and 100 °C in ultra high vacuum conditions for samples treated with 100 ppm of Irgamet®39, in different oils, at 70 °C for 24 hours.

Fig. 8: SSIMS images of: (a) a reference copper sample treated with 100 ppm of Irgamet®39 in Gemini X at 70 °C for 24 hours; (b) a copper sample from the upper part of the winding; (c) a copper sample from the lower part of the winding. The images show: copper (red), sulphur (blue) and tolyltriazole (green). (For interpretation of the references to colour in this figure, the reader is referred to the web version of this article.)

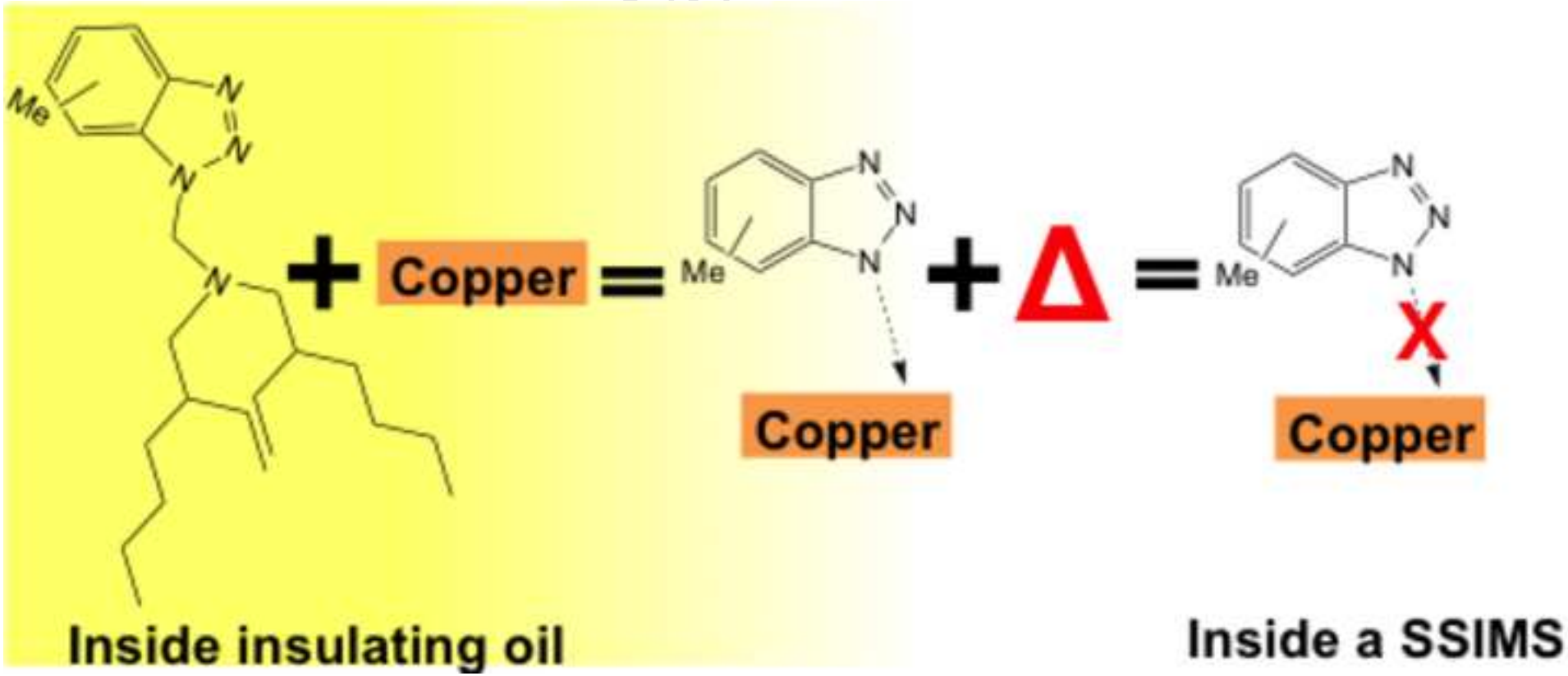
Me
N
N
N
N
+
Copper
=
Me
N
N
N
Copper
+
Δ
=
Me
N
N
N
X
Copper
Inside insulating oil
Inside a SSIMS

Figure 1

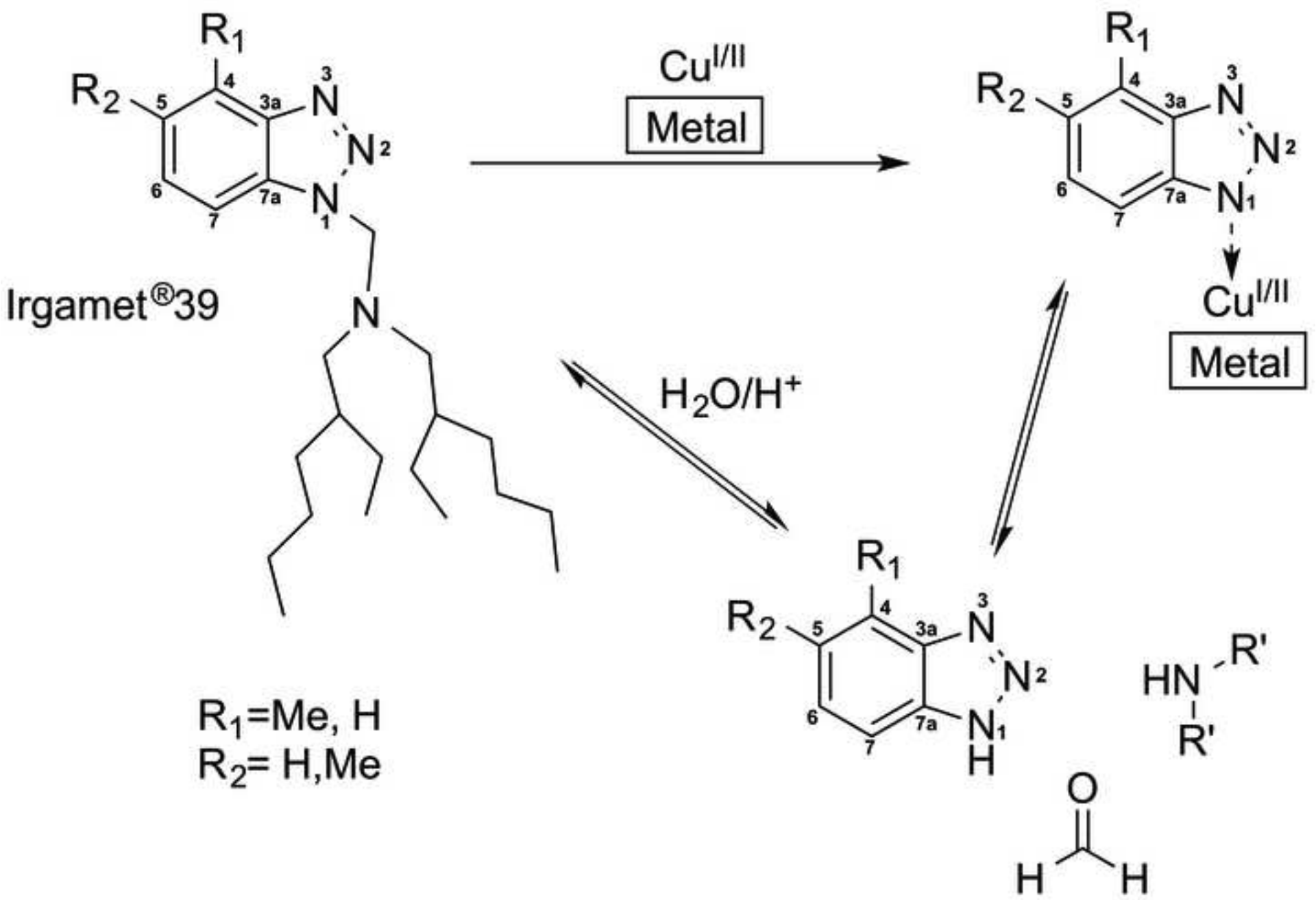
R1
R2
Cu I/II
Metal
Irgamet®39
N
H2O/H+
Cu I/II
Metal
R1=Me, H
R2= H,Me
HN
R'
R'
O
H
H

Figure 2

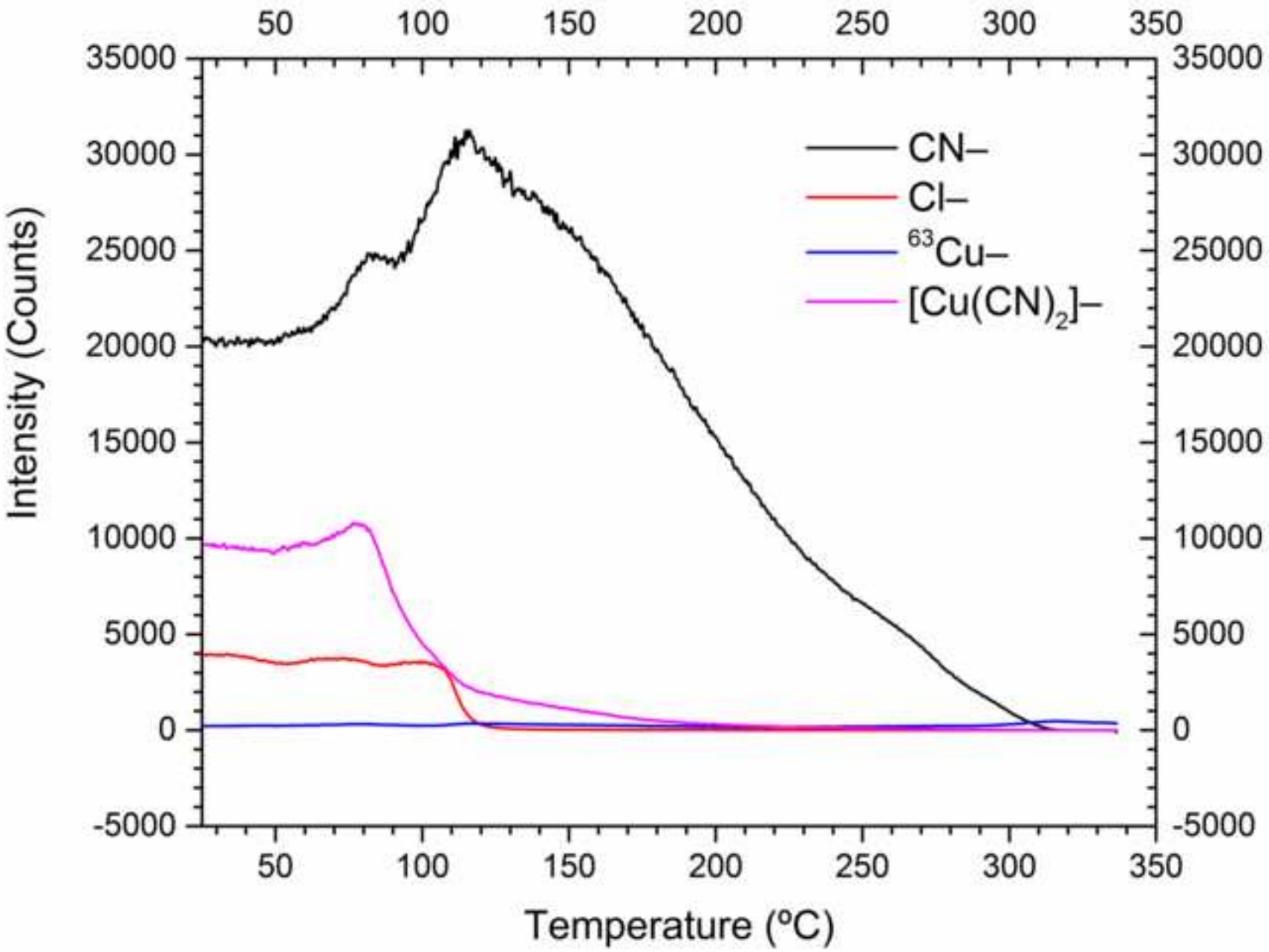
Intensity (Counts)
Temperature (°C)
CN–
Cl–
63Cu–
[Cu(CN)2]–
35000
30000
25000
20000
15000
10000
5000
0
-5000
50
100
150
200
250
300
350

Figure 2 BW

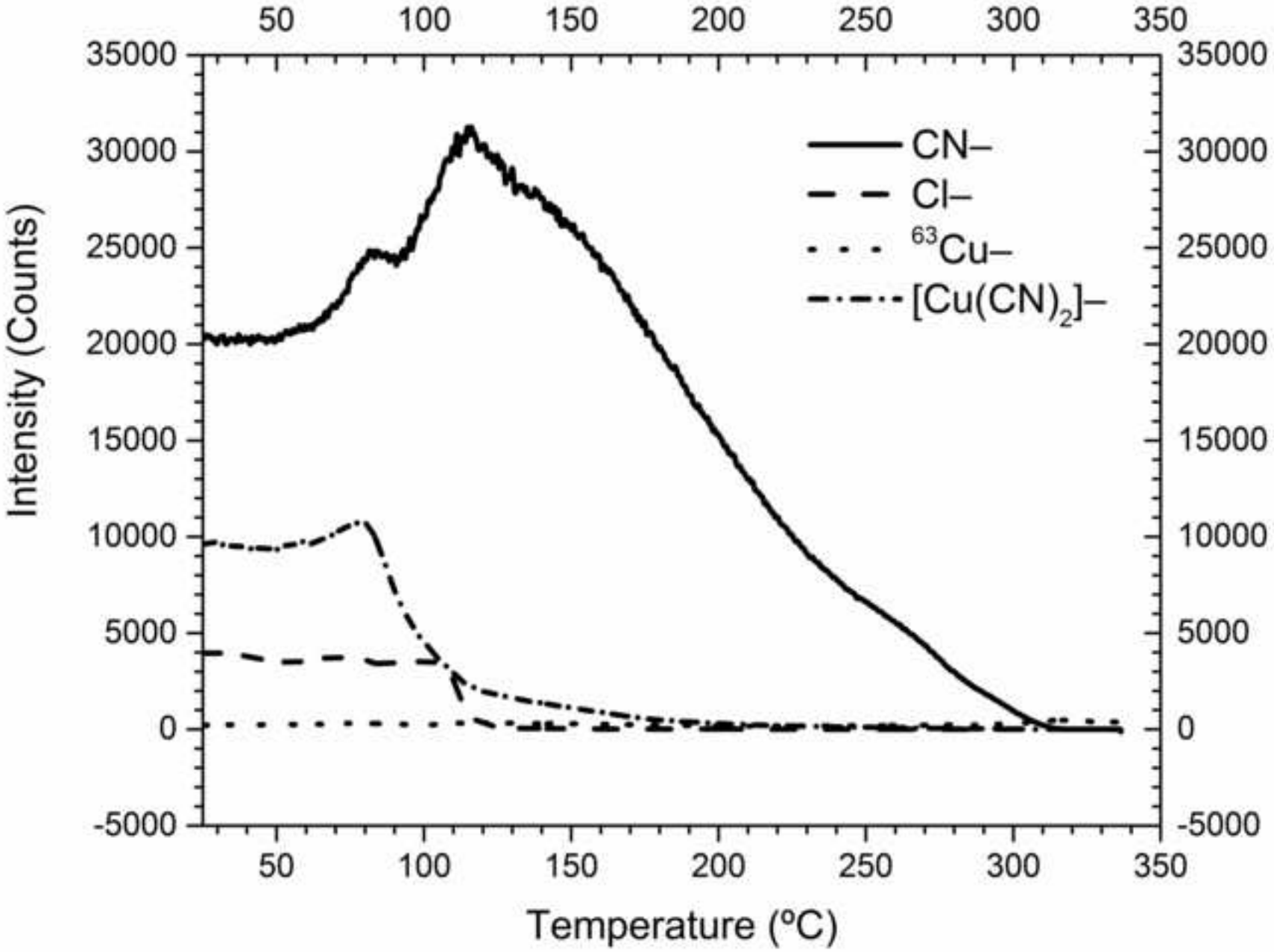
Intensity (Counts)
Temperature (ºC)
CN–
Cl–
63Cu–
[Cu(CN)2]–
35000
30000
25000
20000
15000
10000
5000
0
-5000
50
100
150
200
250
300
350

Figure 3

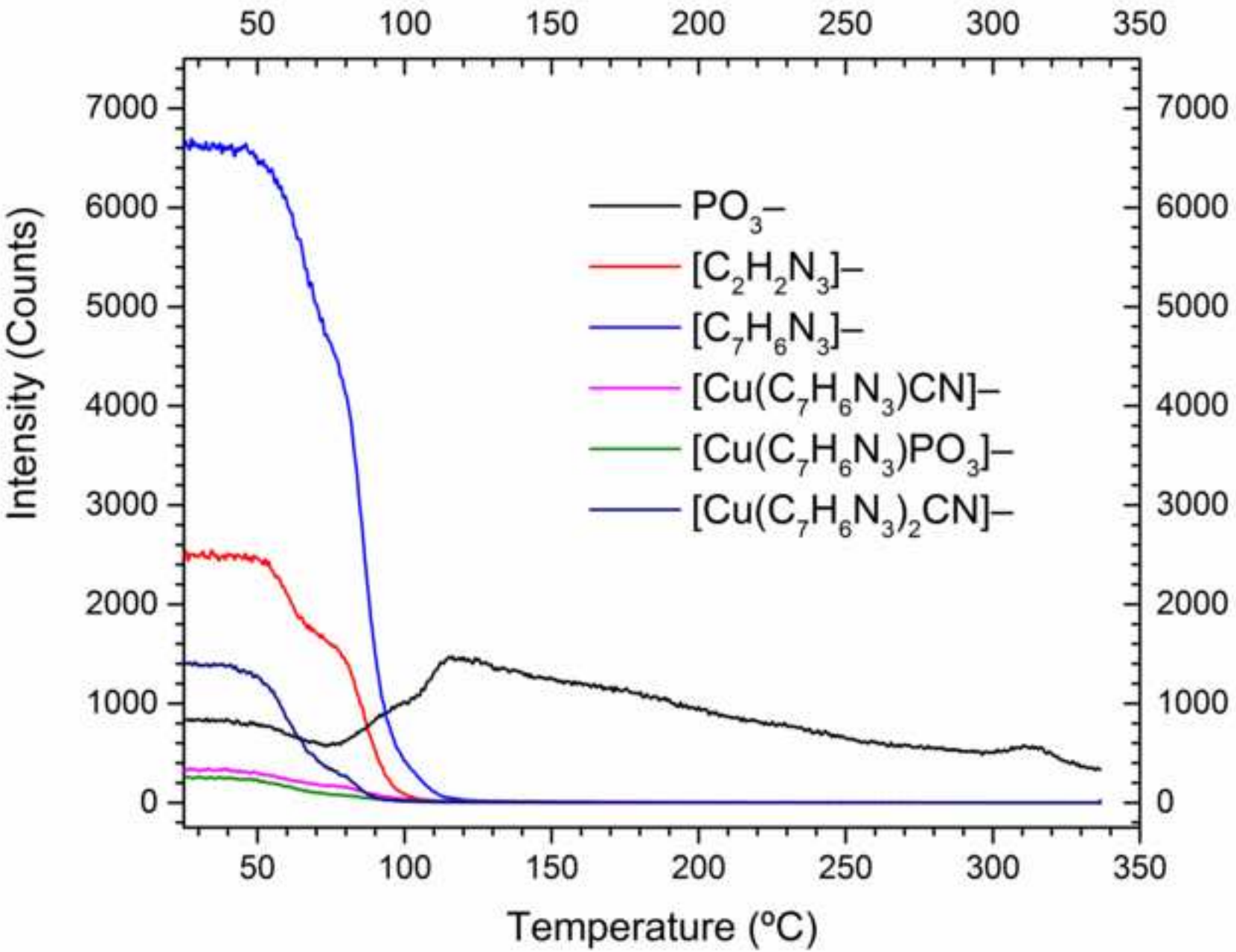
Intensity (Counts)
Temperature (°C)
PO3–
[C2H2N3]–
[C7H6N3]–
[Cu(C7H6N3)CN]–
[Cu(C7H6N3)PO3]–
[Cu(C7H6N3)2CN]–
0
1000
2000
3000
4000
5000
6000
7000
50
100
150
200
250
300
350

Figure 3 BW

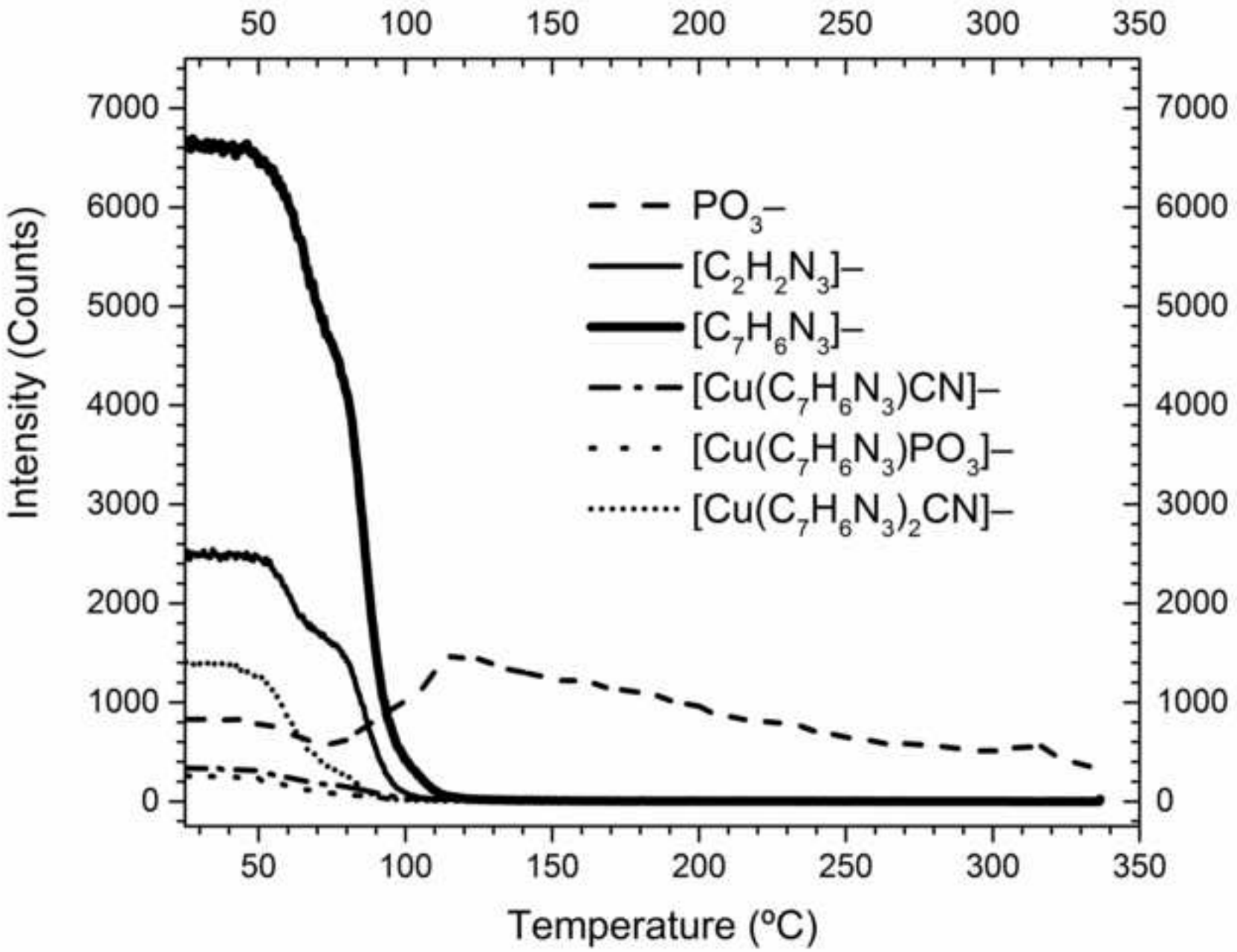
Intensity (Counts)
Temperature (ºC)
PO3–
[C2H2N3]–
[C7H6N3]–
[Cu(C7H6N3)CN]–
[Cu(C7H6N3)PO3]–
[Cu(C7H6N3)2CN]–
0
1000
2000
3000
4000
5000
6000
7000
50
100
150
200
250
300
350

Figure 4

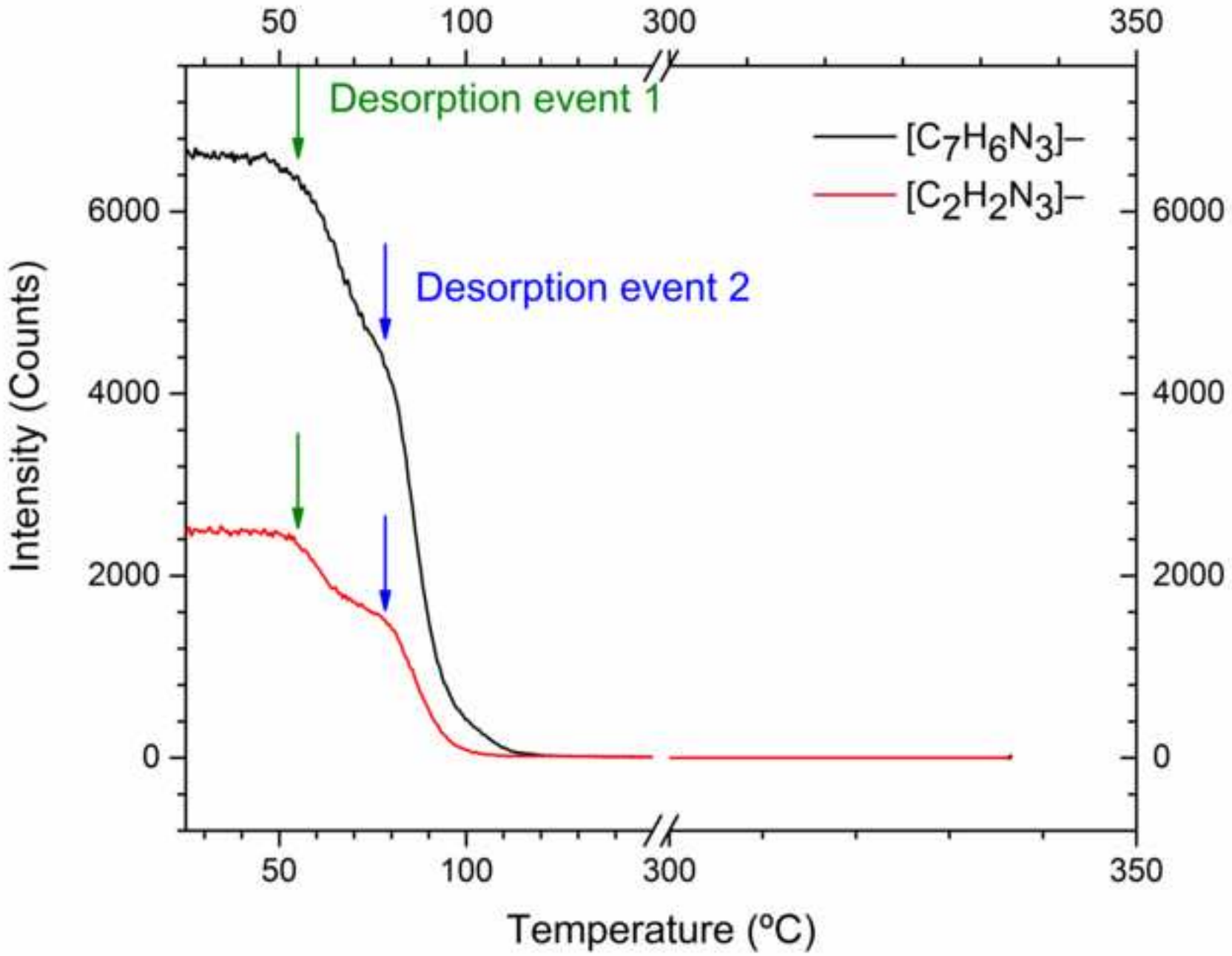
50
100
300
350
Desorption event 1
[C7H6N3]–
[C2H2N3]–
6000
4000
2000
0
Desorption event 2
Intensity (Counts)
Temperature (°C)

Figure 4 BW

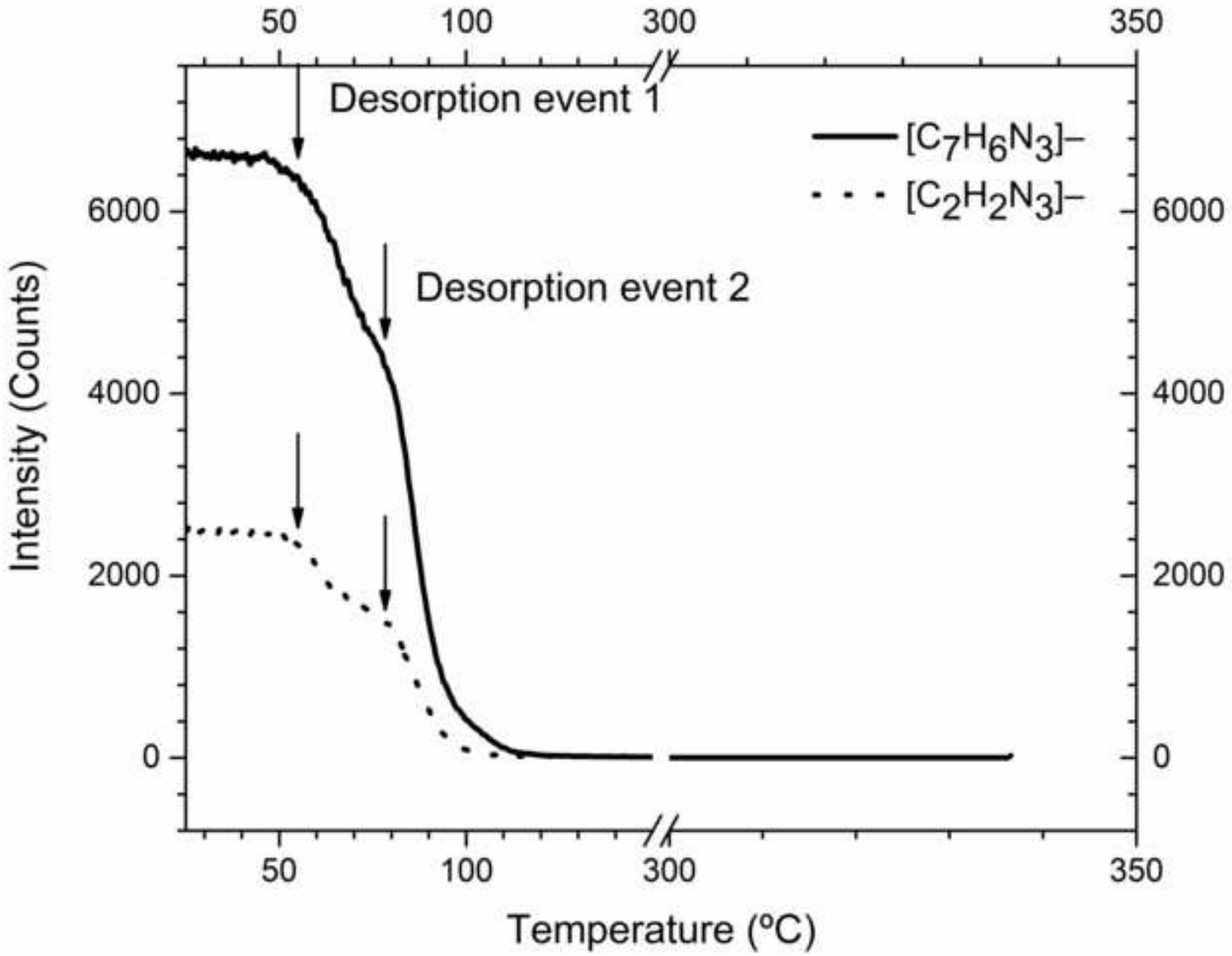
50
100
300
350
Desorption event 1
[C7H6N3]–
[C2H2N3]–
6000
Desorption event 2
4000
2000
0
Intensity (Counts)
Temperature (ºC)

Figure 5

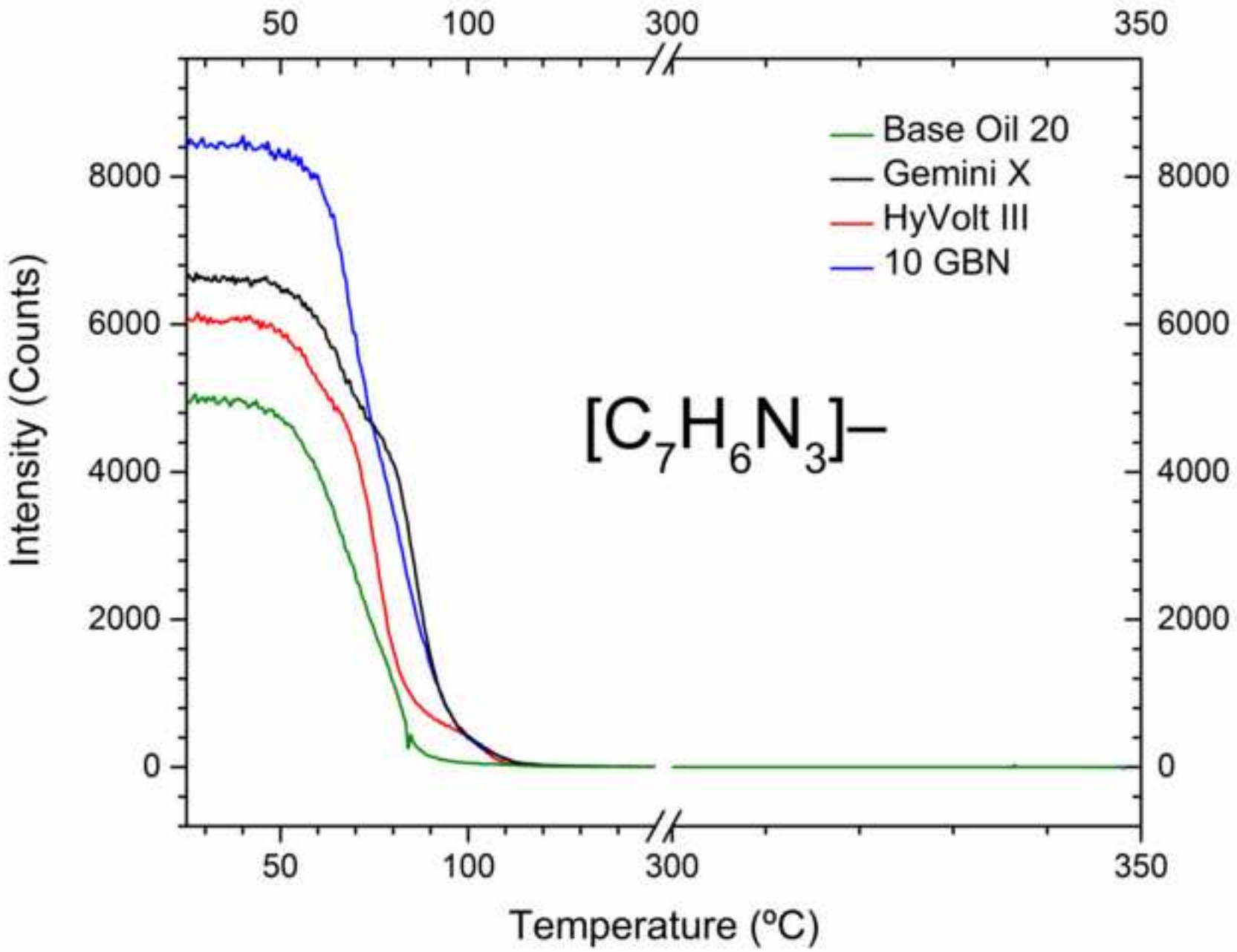
50
100
300
350
8000
6000
4000
2000
0
Intensity (Counts)
Base Oil 20
Gemini X
HyVolt III
10 GBN
[C7H6N3]–
Temperature (ºC)

Figure 5 BW

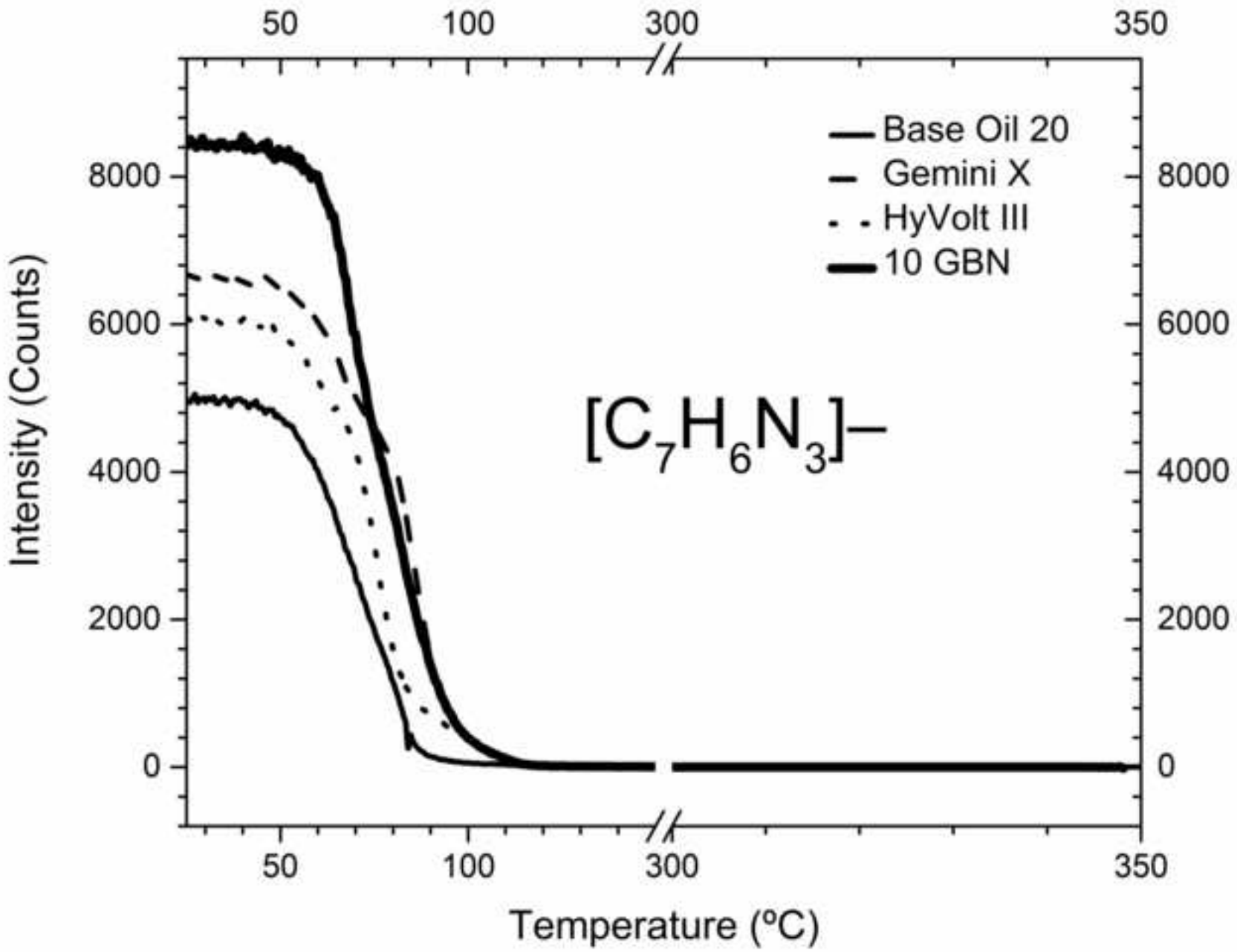
50
100
300
350
Base Oil 20
Gemini X
HyVolt III
10 GBN
8000
6000
4000
2000
0
Intensity (Counts)
[C7H6N3]–
Temperature (ºC)

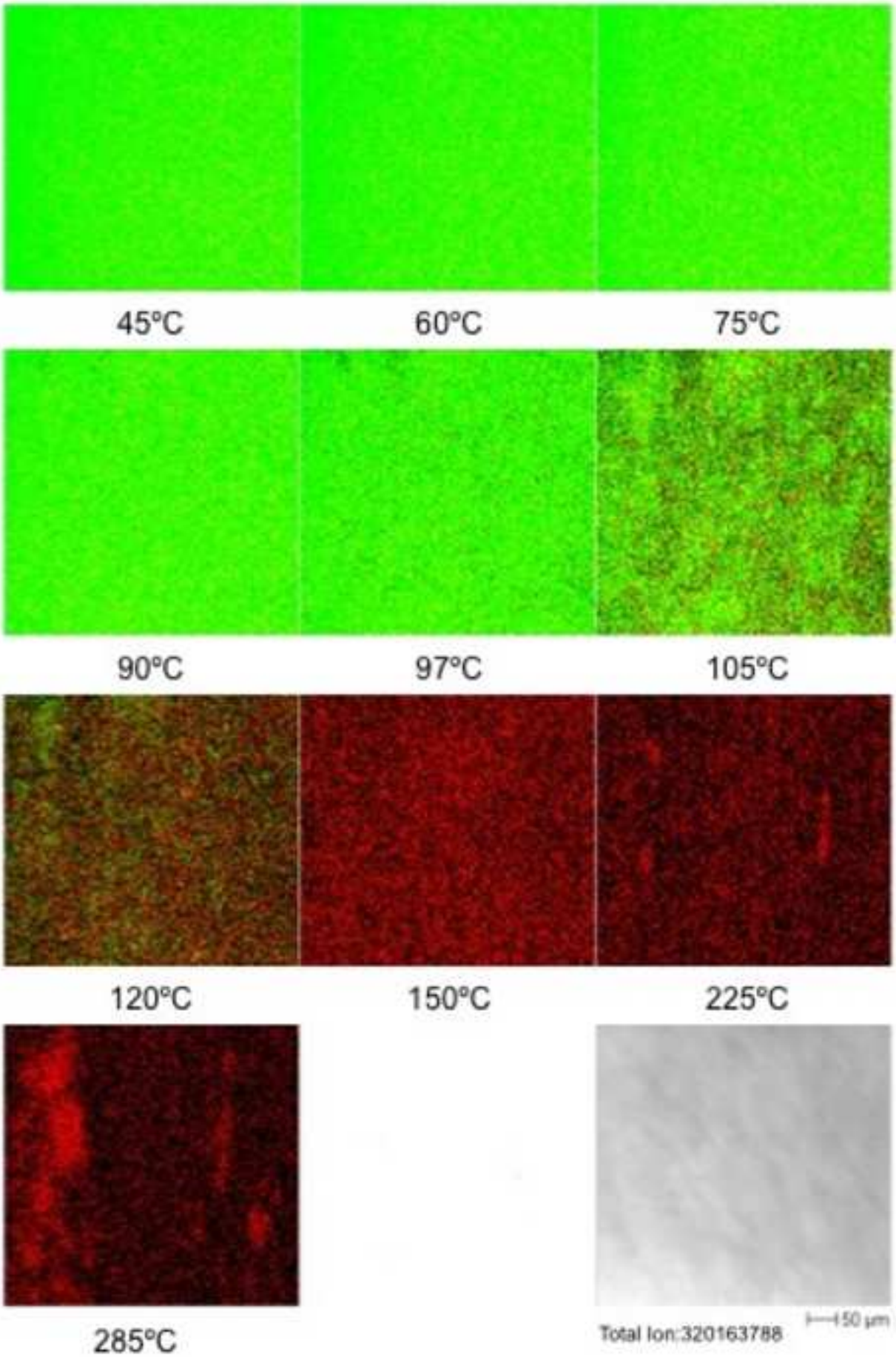

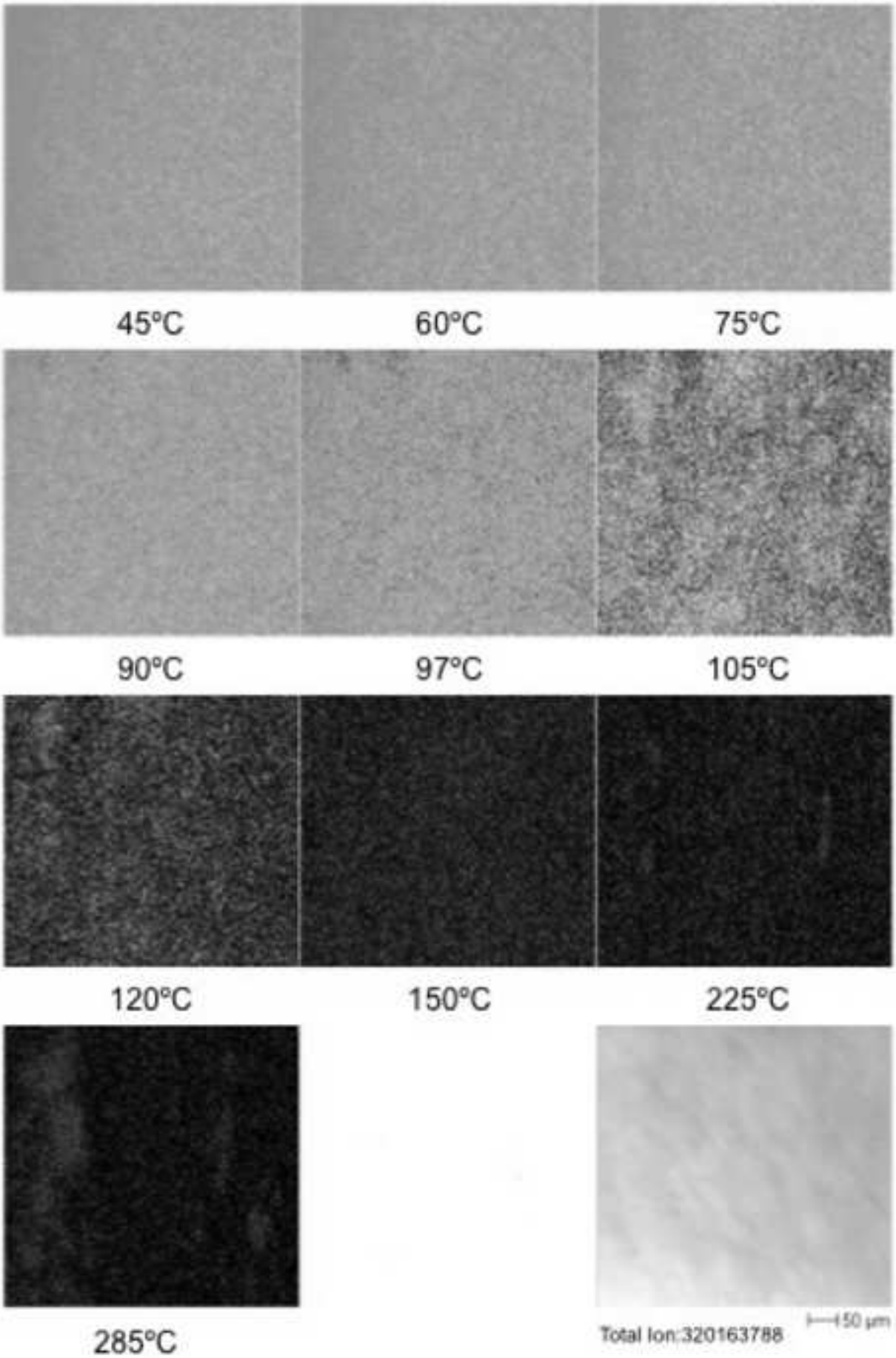

Figure 7

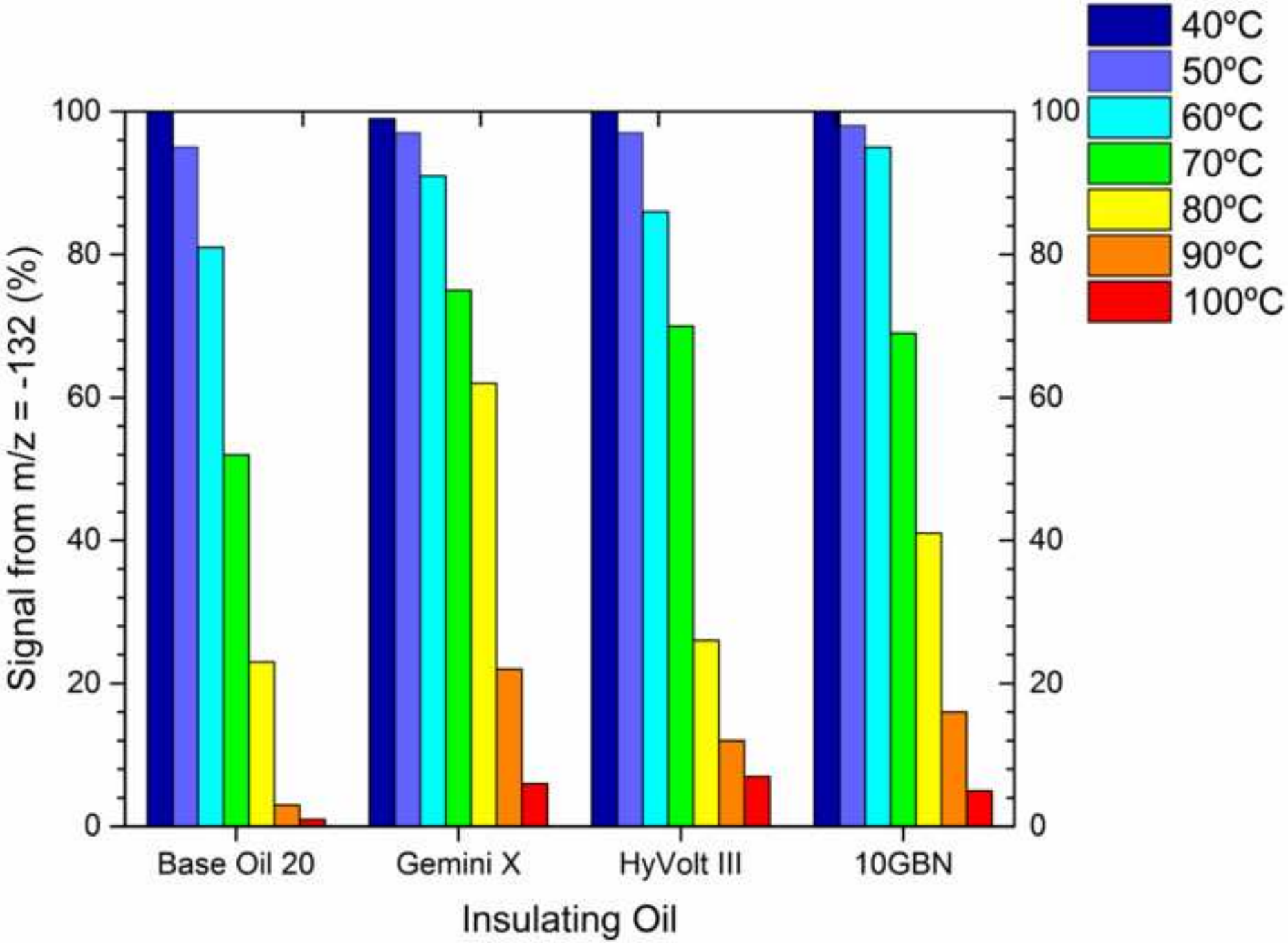
40°C
50°C
60°C
70°C
80°C
90°C
100°C
Signal from m/z = -132 (%)
0
20
40
60
80
100
Base Oil 20
Gemini X
HyVolt III
10GBN
Insulating Oil

Figure 7 BW

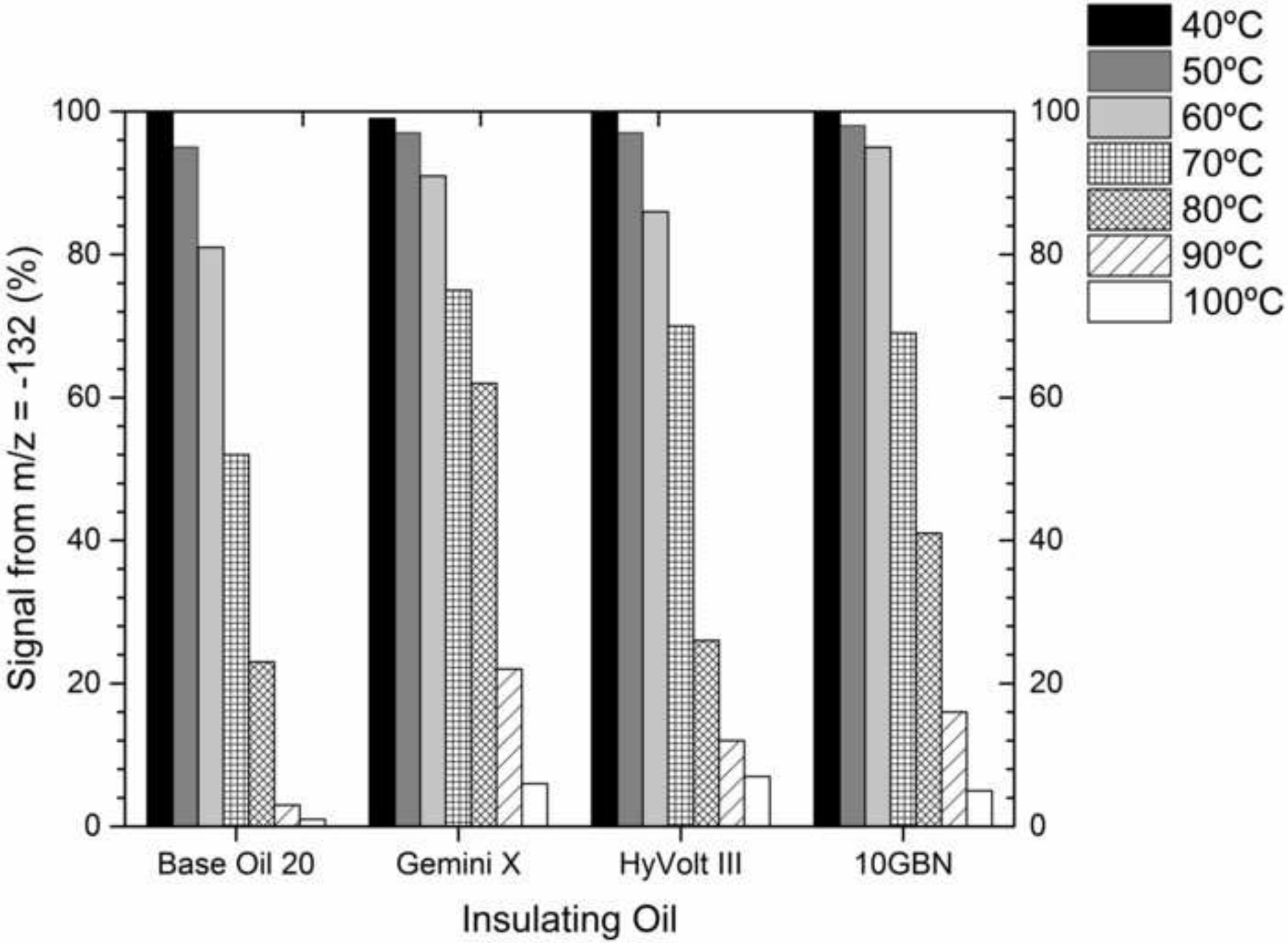
40°C
50°C
60°C
70°C
80°C
90°C
100°C
Signal from m/z = -132 (%)
0
20
40
60
80
100
Base Oil 20
Gemini X
HyVolt III
10GBN
Insulating Oil

Figure 8

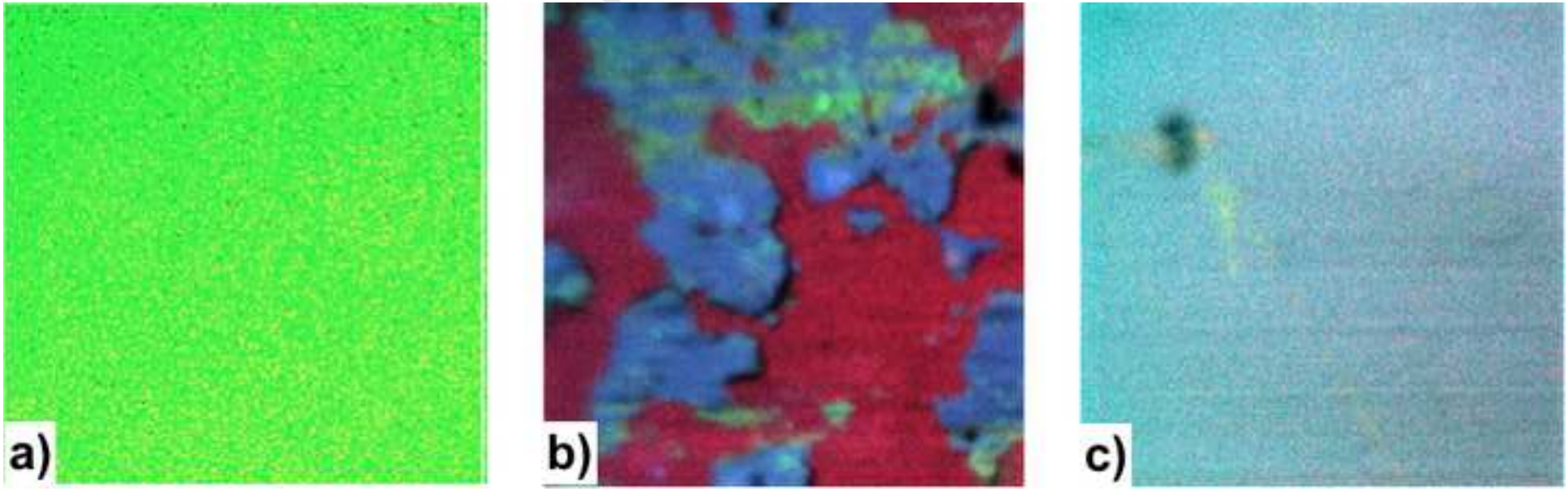

Figure 8 BW